Journal of the Korean Society
for Nondestructive Testing
Vol. 25, No. 3 (2005. 6)

Comparison of Absolute and Differential ECT Signals around Tube Support Plate in Steam Generator

Young-Kil Shin*†, Yun-Tai Lee* and Myung-Ho Song**

Abstract In this paper, absolute and differential eddy current signals from various defects in the steam generator tube are numerically predicted and their signal slope characteristics are investigated. The signal changes due to frequency increase are also observed. After studying signal patterns from various defects and frequencies, the analysis of mixed defect signals affected by the presence of a ferromagnetic support plate is attempted. For the signal prediction, axisymmetric finite element modeling is used and this leads us to the slope angle analysis of the signal. Results show that differential signals are useful for locating the position of a defect under the support plate, while absolute signals are easy to presume and interpret even though the effect of support plate is mixed. Combined use of these two types of signals will help us accomplish a more reliable inspection.

Keywords: ECT, Absolute Signal, Differential Signal, Support Plate, Steam Generator Tube

1. Introduction

For the inspection of steam generator (SG) tubes in a nuclear power plant, the eddy current testing (ECT) is usually employed. However, this method has weakness in inspecting ferromagnetic materials and magnetic saturation is required for a reliable inspection (Cecco et al., 1987; Harvey, 1995). In a certain SG model, ferromagnetic plates are used to support the SG tubes. Crevice gaps are thus formed inevitably between tubes and support plates (SP) and various anomalous defects tend to be developed around them. Therefore, mixed defect signals influenced by the ferromagnetic SP appear in this area and the interpretation of them usually becomes difficult. To predict such complex signals, W. Lord and his collaborators had applied the finite element method based on the variational principle and triangular elements. They predicted differential signals from tube defects near SP (Palanisamy and Lord, 1981) and utilized the method for the design of ECT probe (Ida et al., 1983). In most early works, however, the display of predicted signals did not follow the basis frequency calibration procedure (ASME, 1986) so that they might cause unnecessary confusion. In this paper, predicted signals are displayed following the basis frequency calibration procedure and characteristics of absolute and differential signals obtained from various defects near SP are compared.

2. Finite Element Modeling

When bobbin type differential and absolute probes are used for the inspection of tubular products, axisymmetric finite element modeling is possible if defects are also assumed axisymmetric. This assumption may be justified by the result obtained in the previous study (Lee

Received: April 20, 2005. Accepted: May 30, 2005. * School of Electronic and Information Eng., Kunsan National University, Chonbuk, 573-701, Korea, ** Korea Institute of Nuclear Safety, Yousung-Ku, Taejon, 305-338, Korea, † Corresponding author: ykshin@kunsan.ac.kr

Table 1 Materials and dimensions of tube, support plate, coil and defects [mm]

Tube Outer Diameter	Tube Wall Thickness	Tube / Support Plate Material	Support Plate Thickness	ID defect		OD defect	
				Width	Depth	Width	Depth
19.05	1.3	Inconel 600 / Carbon steel	19.05	1.5	0.26	1.5	0.26
Coil Outer Diameter	Coil Thickness	Coil Width	Coil Spacing	Dent		Bulge	
				Width	Depth	Width	Depth
15.65	1.5	1.5	1.5	4.5	0.13	4.5	0.13

et al., 2000). That is, when the defect depth is fixed and its circumferential length is increased, the slope of differential signal does not change and only the signal magnitude gets bigger. Consequently, the slope angle of the signal becomes the most important criterion to estimate the characteristics of defect. In this work, an axisymmetric finite element code is written based on the Galerkin's Method and isoparametric quadrilateral elements are used (Burnett, 1988). Materials and dimensions of tube, support plate, coil and defects are summarized in Table 1.

3. Signal Display Methods

Differential signal is the trace of differential impedance that results from probe scan and the differential impedance is the difference between the two adjacent coils' impedances. As the leading coil approaches a defect, its impedance changes. But, if the trailing coil's impedance is not yet changed, the signal pattern will be the same as that of the absolute signal. That is, the starting part of a differential signal has the same shape and direction as the corresponding absolute signal (Shin et al., 2004). In this paper, however, they are displayed almost oppositely. This is because differential signals are displayed following the ASME code (ASME, 1986) and absolute signals are rotated so that the fill-factor signal is displayed horizontally (Cecco et al., 1987). According to ASME code, the trace display for the differential signal of the through-the-wall hole should be generated in the directions explained as follows: down and to the right first, followed by an upward motion to the left, followed by a downward motion returning to the point of origin. The slope angle made during this process should be about 40 degrees with the horizontal axis of the display. Based on respective display methods, all the calculated signals are rotated accordingly. Fig. 1 shows the result of such rotation of the differential SP signal obtained at 100 kHz. Noticing x and y components, it is evident that the differential signal starts in the 1st quadrant to the right and upward as the probe approaches the support plate. On the other hand, it can be seen in Fig. 2 that the absolute SP signal at 100 kHz heads for the direction almost opposite (210° or 150°) to the starting direction of the differential signal.

4. Frequency Characteristics of Individual Defect Signals

Fig. 2 and 3 show absolute and differential signals from various defects at frequencies of 100, 300, and 500 kHz. In this paper, signals from 20 % deep inner diameter (ID) and outer diameter (OD) defects, support plate, dent and bulge are predicted and studied. As the frequency increases, the following signal changes are noticed. First, the ID defect signal gets bigger and slightly rotates counterclockwise, but the OD defect signal gets smaller and rotates clockwise rather rapidly. This characteristic can be used to differentiate ID defects from OD defects. Second, the SP signal becomes smaller and rotates clockwise. This is

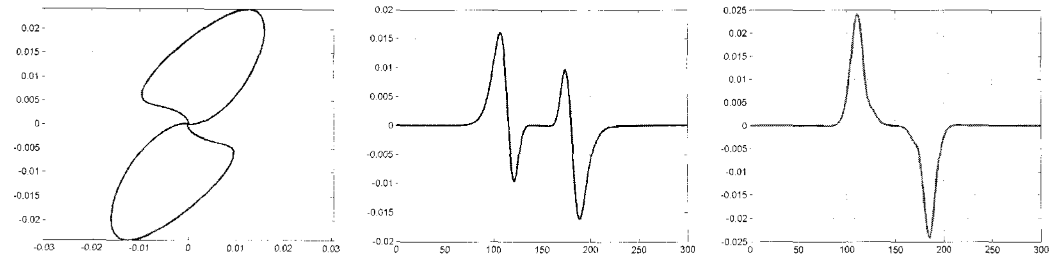

(a) Impedance plane signal (b) X-component signal (c) Y-component signal

Fig. 1 Differential support plate signal displayed according to the ASME code

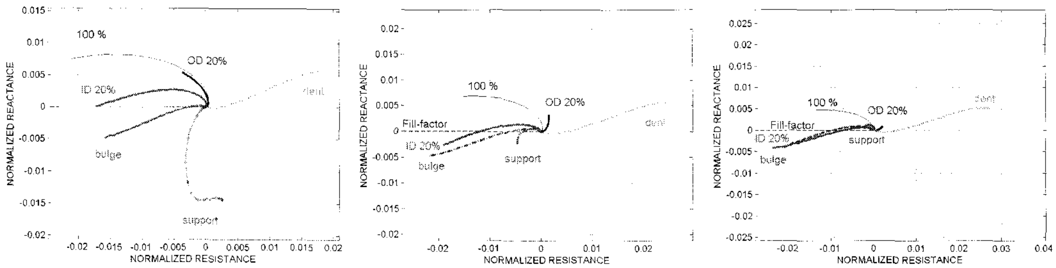

(a) 100 kHz (b) 300 kHz (c) 500 kHz

Fig. 2 Absolute signals from various defects at 3 different frequencies

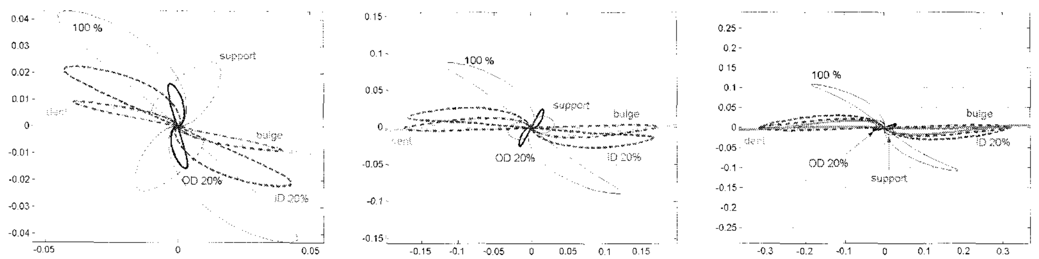

(a) 100 kHz (b) 300 kHz (c) 500 kHz

Fig. 3 Differential signals from various defects at 3 different frequencies

because the SP is ferromagnetic and located outside the tube. Third, the dent and bulge signals become bigger without much rotation as the frequency increases. Dent corresponds to the increase in fill-factor so that its signal appears on the right of horizontal fill-factor signal. On the contrary, bulge corresponds to the decrease in fill-factor so that it yields a signal in the same direction as the decreasing fill-factor signal. However, in the differential signals shown in Fig. 3, the discrimination of the two is very difficult unless their x and y components (or starting directions) are checked.

5. Prediction and Analysis of Mixed Defect Signals affected by Support Plate

After accumulating the knowledge of individual defect signal characteristics, mixed signals that occur when a tube defect is near the

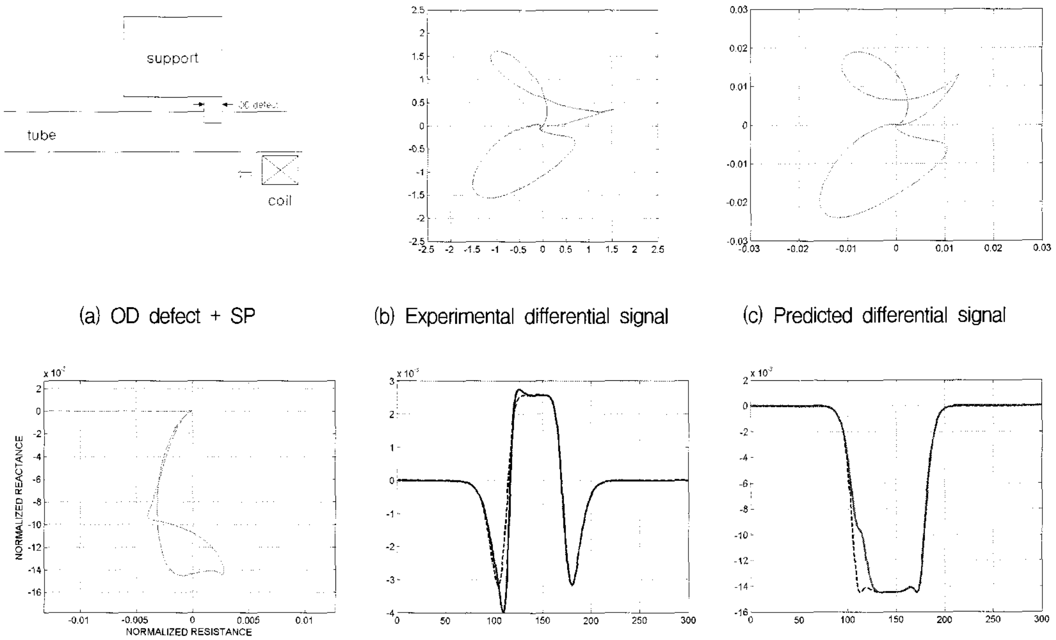

(a) OD defect + SP (b) Experimental differential signal (c) Predicted differential signal

(d) Predicted absolute signal (e) X-component of (d) (f) Y-component of (d)

Fig. 4 Case of an OD defect under the right edge of SP and signals at 100 kHz

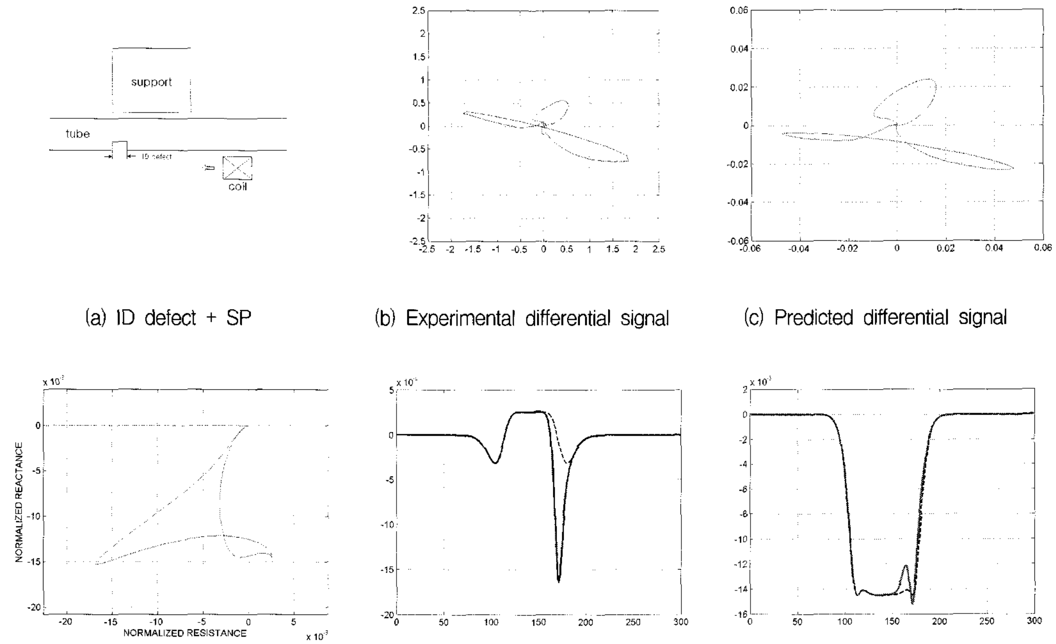

(a) ID defect + SP (b) Experimental differential signal (c) Predicted differential signal

(d) Predicted absolute signal (e) X-component of (d) (f) Y-component of (d)

Fig. 5 Case of an ID defect under the left edge of SP and signals at 100 kHz

ferromagnetic SP are predicted and their signal patterns are investigated. Fig. 4 shows a situation of an OD defect occurred under the right edge of the SP, experimental and predicted differential signals. Predicted absolute signal and its X and Y components are also shown in Fig. 4. Fig. 5 shows a situation of an ID defect occurred under the left edge of the SP and the corresponding signals. In both figures, dotted lines in (e) and (f) represent respective components of the SP signal. The accuracy of predicted signals is confirmed by comparing them with experimental signals. As the probe coil approaches compound defect area as shown in Fig. 4, the starting part of the SP signal changes its pattern and the change appears in the upper right loop of the differential SP signal. On the contrary, if the probe coil meets sound SP first and then a defect under the left edge of the SP as shown in Fig. 5, the starting upper right loop of the differential SP signal does not change and the lower left loop of it changes its shape. Therefore, it can be said that differential signals are useful to locate the position of defect under SP. However, it is very difficult for absolute signals to locate the defect position under SP unless their x and y components are checked. Meanwhile, mixed differential signals shown in Fig. 4 and 5 are difficult to presume or interpret. Mixed absolute signals, however, maintain individual signal characteristics. The slope angle characteristics of SP and OD defect appeared in Fig. 2 are maintained in Fig. 4 and those of SP and ID defect can be seen in Fig. 5. Therefore, it can be said that absolute signals are relatively easier to presume or interpret.

Fig. 6 shows a situation of a bulge occurred under the left edge of the SP and the corresponding signals. Since the difference between bulge and ID defect is on the outer surface of the tube where the influence of coil magnetic fields is weak, their mixed signals are very similar. But, absolute signals may be able to distinguish them using the difference in slope angles of bulge and ID defect signals. Fig. 7 shows a situation of a dent occurred under the

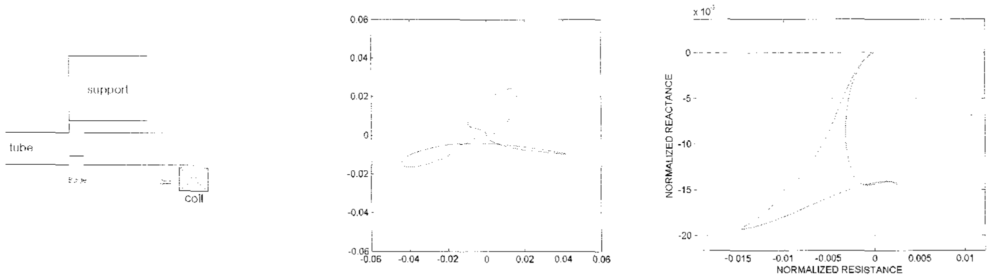

(a) Bulge + SP (b) Differential signal (c) Absolute signal

Fig. 6 Case of a bulge under the left edge of SP and signals at 100 kHz

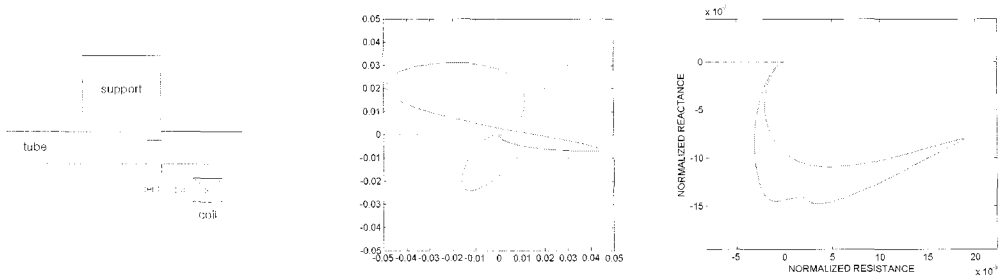

(a) Dent + SP (b) Differential signal (c) Absolute signal

Fig. 7 Case of a dent under the right edge of SP and signals at 100 kHz right edge of the SP and the corresponding signals. In this case, the difference between dent and OD defect is on the inner surface of the tube where the influence of coil magnetic fields is strong. So, their mixed signals are quite different from those in Fig. 4.

Fig. 8 shows signals obtained at 300 kHz from OD and ID defects that are located under the left edge of SP. In the mixed OD defect signals, signal portions due to defect and SP are

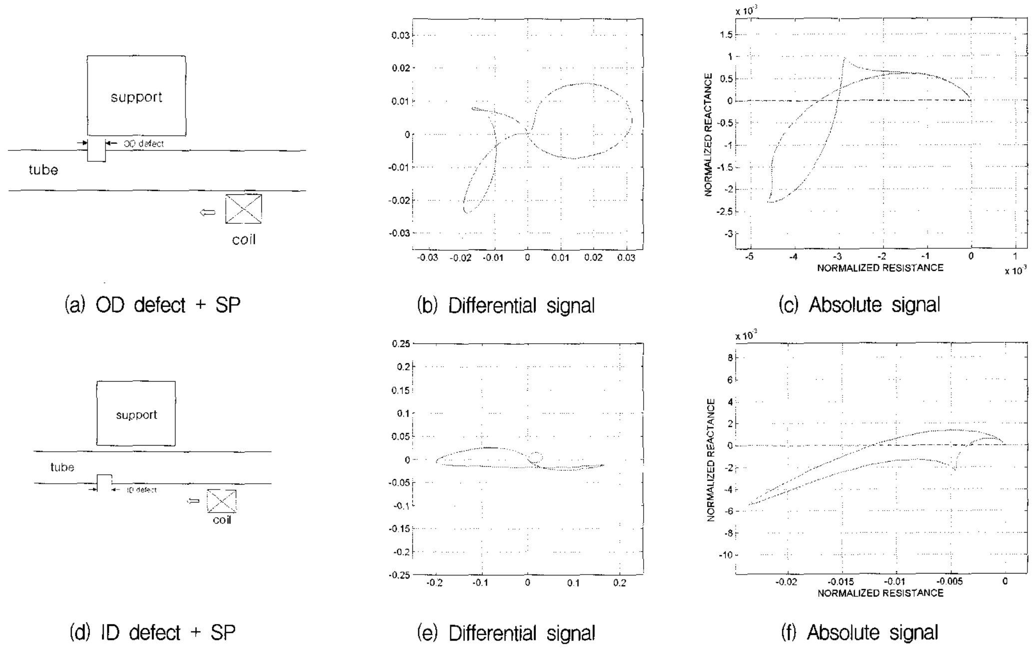

(a) OD defect + SP (b) Differential signal (c) Absolute signal

(d) ID defect + SP (e) Differential signal (f) Absolute signal

Fig. 8 Cases of OD and ID defects under the left edge of SP and signals at 300 kHz

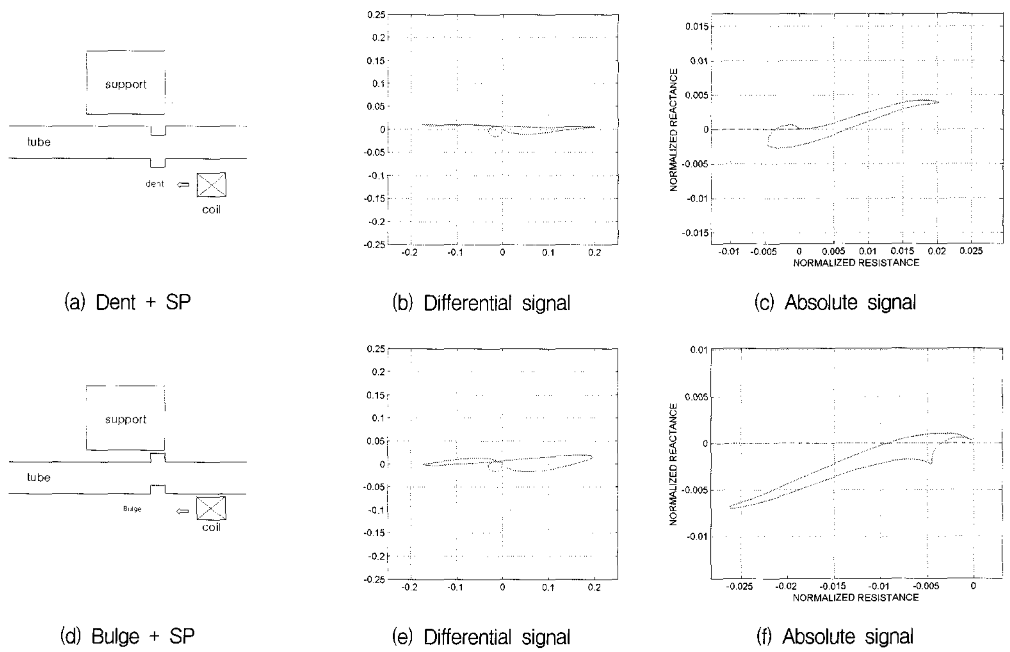

(a) Dent + SP (b) Differential signal (c) Absolute signal

(d) Bulge + SP (e) Differential signal (f) Absolute signal

Fig. 9 Cases of a dent and a bulge under the right edge of SP and signals at 300 kHz

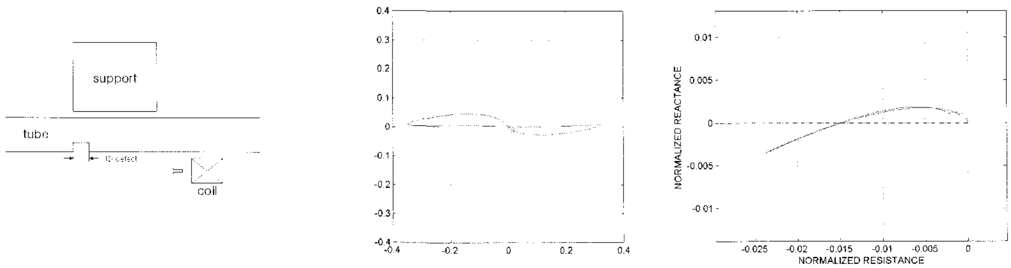

(a) ID defect + SP (b) Differential signal (c) Absolute signal

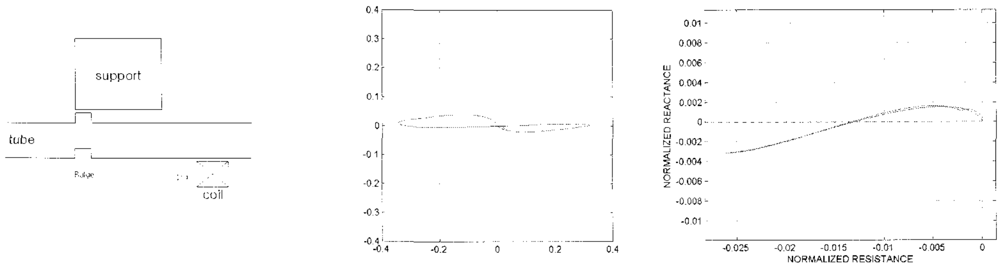

(d) Bulge + SP (e) Differential signal (f) Absolute signal

Fig. 10 Cases of an ID defect and a bulge under the left edge of SP and signals at 500 kHz

of comparable size. In the mixed ID defect signals, however, the signal portion due to ID defect is larger than that of SP since the defect is closer to the coil's magnetic fields. Fig. 9 shows signals obtained at 300 kHz when a dent and a bulge are under the same right edge of SP. Differential signals are not easy to distinguish them unless their x and y components are checked. However, it is very simple for absolute signals to distinguish them since the starting directions of the two signals are opposite.

In Fig. 10, the influence of SP is effectively removed by choosing the higher frequency. However, at 500 kHz, mixed ID defect and bulge signals are not distinguishable in both differential and absolute signals. This is because the separation angle between ID defect and bulge signals gets reduced as the frequency is increased. This can be seen in Fig. 2 and 3. Therefore, it would be better to use a low frequency as shown in Fig. 5 and 6 if the objective of test is to distinguish ID defect from bulge.

6. Summary

In this paper, mixed ECT signals that occur when a tube defect is near the ferromagnetic support plate are predicted and their patterns are analyzed. At first, signals from various anomalous defects are investigated. Their slope characteristics and frequency dependent behavior are observed. After that, mixed signals are predicted and carefully observed how the characteristic of individual defect signal is mixed into them.

Judging by the impedance plane signals, absolute signals are easy to presume and interpret even though they are mixed and differential signals are useful to locate the position of defect under the support plate. To distinguish a dent from a bulge, horizontal and vertical components of the differential signal must be checked, while it is very simple for the absolute signal to distinguish them. To locate the position of a defect under the support plate, however, horizontal and vertical components of the absolute signal must be checked out. Thus, one type of signal has merits over the other for a certain case, but it has also demerits in another situation. Therefore, combined use of these two types of signals would be helpful for more reliable defect characterization.

Acknowledgment

This work has been supported by SAFE(Safe and Structural Integrity Research Center), which is funded by KOSEF(Korea Science and Engineering Foundation).

References

ASME (1986) *Eddy Current Examination Method for Installed Nonferromagnetic Steam Generator Heat Exchanger Tubing*, Section V, Article 8, Appendix I

Burnett, D. S. (1988) *Finite Element Analysis from Concepts to Applications*, Addison-Wesley, Reading, Massachusetts, USA

Cecco, V. S., Drunen, G. V. and Sharp, F. L. (1987) *Eddy Current Testing*, GP courseware, Columbia, MD, USA, pp. 8-142

Harvey, E. D. (1995) *Eddy Current Testing Theory and Practice*, ASNT, USA, pp. 15-52

Ida, N., Palanisamy, R. and Lord, W. (1983) Eddy Current Probe Design Using Finite Element Analysis, *Materials Evaluation*, Vol. 41, No. 11, pp. 1389-1394

Lee, H. B., Won, S. Y. and Shin, Y. K. (2000) Finite Element Analysis of Eddy Current Testing for Tubes with 3-Dimensional Defects", *Journal of the Korean Society for Nondestructive Testing*, Vol. 20, No. 3, pp. 191-199

Palanisamy, R. and Lord, W. (1981), Finite Element Simulation of Support Plate and Tube Defect Eddy Current Signals in Steam Generator NDT", *Materials Evaluation*, Vol. 39, No. 7, pp. 651-655

Shin, Y. K., Lee, Y. T., Lee, J. H. and Song, M. H. (2004) Drawing of Impedance Plane Diagrams of Absolute Coil ECT Signals by Finite Element Analysis, *Journal of the Korean Society for Nondestructive Testing*, Vol. 24, No. 4, pp. 315-324